

# fastatomstruct: A High-Performance Library for Structural and Dynamical Analysis of Atomic Systems

Nils Holle<sup>1</sup>, Sebastian Walfort<sup>1</sup>, Riccardo Mazzarello<sup>2</sup>, and Martin Salinga<sup>1</sup>

<sup>1</sup> University of Münster, Institute of Materials Physics, Germany <sup>2</sup> Sapienza Università di Roma

DOI: [10.21105/joss.08106](https://doi.org/10.21105/joss.08106)

## Software

- [Review](#)
- [Repository](#)
- [Archive](#)

Editor: [Christoph Junghans](#)

## Reviewers:

- [@tukss](#)
- [@markcmiller86](#)

Submitted: 24 February 2025

Published: 26 June 2025

## License

Authors of papers retain copyright and release the work under a

Creative Commons Attribution 4.0 International License ([CC BY 4.0](#)).

## Summary

fastatomstruct is a Python library, implemented primarily in Rust, designed to efficiently calculate a wide range of atomic structural and dynamical parameters. Using thread-based parallelization via Rust's rayon crate, the package provides fast and scalable performance for analyzing atomic configurations. In particular, many functions in this library are targeted at the structural and dynamical analysis of large liquid, supercooled-liquid, and amorphous systems. Its primary audience includes researchers in computational materials physics, materials science, and chemistry, though it is also broadly applicable to any field requiring detailed structural analysis of atomic systems.

The library provides a comprehensive suite of tools for analyzing atomic configurations, supporting the calculation of radial distribution functions, static structure factors, bond-orientational parameters, and vibrational density of states, among others. By leveraging MPI-based parallelization (`mpi4py`) alongside Rust's rayon crate for thread-based parallelization, fastatomstruct achieves high efficiency, making it particularly useful for large-scale simulations.

## Statement of need

Understanding atomic structure and dynamics is fundamental in many scientific disciplines, including the study of phase transitions, the behavior of supercooled liquids, and the exploration of molecular interactions. Answering many questions in these fields requires simulations of large systems. Today, this is possible with quantum mechanical accuracy using machine-learned potentials (Friederich et al., 2021). However, efficiently calculating structural quantities from large atomic simulations can be computationally expensive. Existing tools often lack support for high-performance parallelization or the ability to integrate seamlessly with Python-based analysis workflows, such as those built around the widely used Atomic Simulation Environment (ASE) (Hjorth Larsen et al., 2017).

fastatomstruct addresses this gap by offering a Rust-backed implementation with efficient parallelization techniques that exploit multicore processors and thread-based parallelization. This allows researchers to investigate a wide range of atomic-scale phenomena. In materials science, the library facilitates the study of phase transitions, e.g. crystallization or melting, by tracking bond-orientational parameters and radial distribution functions, providing insights into how atomic structures evolve under changing conditions. In condensed matter physics and engineering, it enables the characterization of atomic defects, local structural distortions, and vibrational properties, aiding in the design of materials with specific desired properties. The library is particularly useful in the study of soft matter and supercooled liquids, where non-Gaussian transport behavior, mean squared displacement, and velocity autocorrelation functions help uncover the fundamental mechanisms of glassy dynamics. Furthermore, fastatomstruct provides tools for analyzing molecular structure through three-body correlations and other

structural parameters that go beyond the traditional two-body quantities like pair radial distribution functions.

The library's scalability makes it particularly suited for analyzing large datasets. For instance, computing the coordination numbers of a bulk structure containing half a million atoms can be completed in approximately 0.3 seconds on 96 cores (see Figure 2), demonstrating its ability to handle high-throughput simulations efficiently. Figure 1 shows a comparison of a radial distribution function calculation using fastatomstruct and the widely used MDAnalysis Python library. The calculations yield equivalent results, but fastatomstruct is approximately 20 times faster due to its parallelized implementation. In comparison to other commonly used packages such as MDAnalysis (Gowers et al., 2016; Michaud-Agrawal et al., 2011), pymatgen (Ong et al., 2013), or functions built into ASE, fastatomstruct distinguishes itself through its high-performance design and scalability. Its Rust-based core leverages advanced thread and MPI parallelization strategies to achieve substantially faster processing of large datasets, while ensuring memory and thread safety. Easy installation and a direct integration with Python workflows and established tools like ASE further streamlines its usage, avoiding the complexity often encountered with other codes.

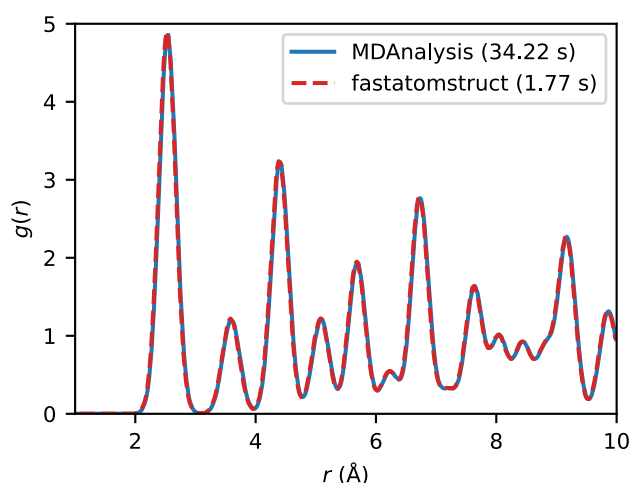


**Figure 1:** Comparison of radial distribution function calculation between fastatomstruct and MDAnalysis shows a 20× speedup with the parallelized implementation in fastatomstruct. The RDF was calculated for a copper crystal with 108,000 atoms. Calculations were performed on two Intel Xeon Gold 6140 processors with a total of 36 cores and threads. The speedup is mainly due to the parallelization of distance calculations. Note that we do not observe an ideal 36× speedup as a) the simple distance calculations required for the computation of the radial distribution function do not scale as well as the calculation of more complex quantities like bond order correlation parameters (see Figure 3), b) some calculation time is spent on the non-parallelized creation of the histogram, and c) there is overhead due to the dual-processor setup.

## Features and background

The `fastatomstruct` library calculates a variety of structural quantities that provide insights into atomic arrangements. **Distances between atoms** are calculated using a linear scaling method (see Figure 2), which also allows for fast calculations of quantities like coordination numbers. Spatial hashing enables efficient neighbor finding and distance calculations with  $\mathcal{O}(N)$  scaling instead of the  $\mathcal{O}(N^2)$  complexity of naive all-pairs approaches. This algorithm divides the simulation box into a regular grid of cells, where each cell has dimensions larger than the maximum interaction cutoff radius. Each atom's coordinates are converted into a cell index using a hash function based on discretized spatial coordinates - hence the term "spatial hashing". Atoms are assigned to cells based on these hashed coordinates, and neighbor searches only consider atoms within the same cell and its neighboring cells. For large systems, this dramatically reduces the number of pairwise distance calculations required.

The **coordination number** is the number of atoms within a defined cutoff distance  $r_{\text{cut}}$  of a reference atom. It is computed as

$$\text{CN} = \sum_j \Theta(r_{\text{cut}} - |\mathbf{r}_i - \mathbf{r}_j|),$$

where  $\Theta(x)$  is the Heaviside step function. The **radial distribution function**,  $g(r)$ , quantifies the probability of finding a particle at a distance  $r$  from a reference particle. It is defined as

$$g(r) = \frac{dn_r}{4\pi\rho r^2 dr},$$

where  $dn_r$  is the number of atoms in a shell of thickness  $dr$  at a distance  $r$  from the reference atom, and  $\rho$  is the atomic number density. The implementation constructs a histogram using rectangular window function binning, with efficient neighbor finding through spatial hashing. The resulting histogram is normalized by the shell volume and bulk density to obtain the distribution function. The **static structure factor**,  $S(q)$ , which is derived from the radial distribution function, describes the spatial correlations in the system and is given by

$$S(q) = 1 + 4\pi\rho \int_0^\infty r^2 [g(r) - 1] \frac{\sin(qr)}{qr} dr,$$

where  $\rho$  is again the atomic number density and  $q$  is the magnitude of the scattering vector. `fastatomstruct` further implements statistics of bond angles

$$\cos \theta_{ijk} = \frac{\mathbf{r}_{ij} \cdot \mathbf{r}_{ik}}{r_{ij}r_{ik}},$$

yielding the **bond angle distribution**. The implementation identifies all triplets of atoms where the central atom has two neighbors within a cutoff distance, computes the angle between the bond vectors using the dot product formula, and constructs a histogram of these angles.

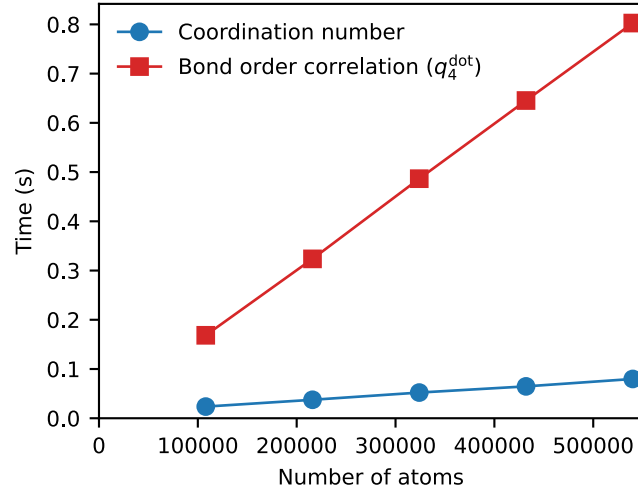


**Figure 2:** Linear scaling of distance calculations in fastatomstruct allows for efficient computation of structural quantities. The distance between atoms is calculated using spatial hashing, which divides the simulation box into cells and only considers atoms within neighboring cells. The calculations have been performed on an AMD EPYC Genoa 9654 processor with 96 cores and threads.

fastatomstruct also includes implementations of a higher-order correlation function, the **three-body correlation** (TBC) (Ronneberger et al., 2016). The TBC quantifies the spatial correlations between triplets of atoms and is useful for capturing repeating geometric motifs in atomic configurations. It is defined as

$$g^{(3)}(r_1, r_2) = \frac{V}{\rho(N-1)(N-2)} \sum_{i_1, i_2, i_3} \langle \delta(r_1 - r_{i_1 i_2}) \delta(r_2 - r_{i_2 i_3}) \rangle,$$

with  $i_1$ ,  $i_2$  and  $i_3$  distinct indices of atoms,  $V$  the unit cell volume,  $N$  the number of particles, and  $\rho = V/N$  the atomic density. The average runs over time. The implementation constructs a two-dimensional histogram by binning pairs of distances  $(r_1, r_2)$  for all connected triplets of atoms, using efficient neighbor finding to identify triplets and delta function approximation through histogram binning. The related **angular-limited three-body correlation** ALTBC (Bichara et al., 1993) is particularly relevant in the context of Peierls-like distortions, which here refers to alternating chains of long and short bonds in either disordered or ordered systems. The ALTBC again quantifies the spatial correlations between triplets of atoms, where the angles between pairs are constrained to lie within a specified range. It is defined as

$$g_{\text{AL}}^{(3)}(r_1, r_2) = \frac{V}{\rho(N-1)(N-2)} \sum_{i_1, i_2, i_3} \langle \delta(r_1 - r_{i_1 i_2}) \delta(r_2 - r_{i_2 i_3}) \Theta(\beta - \delta) \rangle,$$

with

$$\cos \beta = \frac{\vec{r}_{i_1 i_2} \cdot \vec{r}_{i_2 i_3}}{r_{i_1 i_2} r_{i_2 i_3}}$$

the alignment angle.  $\delta$  specifies the range of angles included in the calculation of the ALTBC. The implementation extends the standard TBC by adding an angular constraint, computing the bond angle for each triplet and applying the Heaviside step function to include only triplets within the specified angular range. The **bond length ratio** allows to quantify the information contained in the ALTBC in a single number. It is defined in analogy to the ALTBC as (Holle et al., 2025)

$$\text{ALBLR} = \frac{\sum_{i_1, i_2, i_3} \frac{\max(r_{12}, r_{23})}{\min(r_{12}, r_{23})} \Theta(\beta - \delta) \bar{\Theta}(r_{12}) \bar{\Theta}(r_{23})}{\sum_{i_1, i_2, i_3} \Theta(\beta - \delta) \bar{\Theta}(r_{12}) \bar{\Theta}(r_{23})}.$$

The implementation computes the ratio of maximum to minimum bond lengths for each triplet, applies the angular constraint through the step function, and normalizes by the number of qualifying triplets to obtain an average bond length ratio that characterizes local structural distortions.

**Bond-orientational parameters**, originally introduced by Steinhardt et al. (Steinhardt et al., 1983), quantify the local angular symmetry around atoms. These parameters help distinguish between different phases, such as liquids and crystals. They are computed using spherical harmonics  $Y_{lm}(\theta, \phi)$ , with the  $q_l$  parameter given by

$$q_l = \sqrt{\frac{4\pi}{2l+1} \sum_{m=-l}^l |q_{lm}|^2},$$

where  $q_{lm}$  is the average spherical harmonic for neighbors around a reference particle. The implementation applies smooth radial cutoff functions to weight neighboring atoms, and efficiently sums over neighboring particles identified through spatial hashing. These parameters are widely used to characterize the structural order in liquids and glasses. The local averages are given by

$$q_{lm}(i) = \frac{1}{N_i^{\text{eff}}} \sum_j f(r_{ij}) Y_{lm}(\hat{r}_{ij}),$$

where  $\hat{r}_{ij}$  denotes the normalized distance vector between atoms  $i$  and  $j$ .  $f(r)$  is the radial cutoff function, which is defined as

$$f(r) = \frac{1 - (r/r_{\text{cut}})^{p_1}}{1 - (r/r_{\text{cut}})^{p_2}},$$

with the cutoff radius  $r_{\text{cut}}$  and additional parameters  $p_1$  and  $p_2$ . For  $p_1 \rightarrow \infty$  and  $p_2 \rightarrow \infty$ , this function becomes a sharp cutoff.  $N_i^{\text{eff}}$  is the effective coordination number

$$N_i^{\text{eff}} = \sum_j f(r_{ij}).$$

**Bond order correlation parameters** are particularly effective at discriminating between ordered (crystalline) and disordered (amorphous) environments. “Bond order correlation” here refers to the correlation between bond orientational parameters. They are defined as (Ronneberger et al., 2016)

$$q_l^{\text{dot}}(i) = \frac{1}{N_i^{\text{eff}}} \sum_j f(r_{ij}) C_{ij}.$$

The implementation first calculates the normalized bond-orientational parameters for each atom, then computes the complex dot product between neighboring atoms' parameters to obtain the correlation coefficient  $C_{ij}$ , which quantifies the similarity in local orientational order. Here,

$$C_{ij} = \sum_{m=-l}^l \frac{q_{lm}(i) q_{lm}^*(j)}{\sqrt{\sum_m |q_{lm}(i)|^2} \sqrt{\sum_m |q_{lm}(j)|^2}}$$

are the bond order correlators (ten Wolde et al., 1995). The  $q_{lm}(i)$  are again the local averages of spherical harmonics as given above.

To quantify the local **tetrahedral order** in atomic configurations, the library also provides the tetrahedral order parameter  $q_{\text{tetrahedral}}$ , which is defined as (Duboué-Dijon & Laage, 2015; Lee et al., 1993)

$$q_{\text{tetrahedral}} = 1 - \frac{3}{8} \sum_{i>k} \left( \frac{1}{3} + \theta_{ijk} \right)^2.$$

Here, the sum runs over all pairs of atoms bonded to a central atom  $j$  and forming a bond angle  $\theta_{ijk}$ . The parameter is calculated for a fixed number  $N$  of nearest neighbors. The

implementation identifies the  $N$  nearest neighbors of each atom, computes all pairwise bond angles between these neighbors, and evaluates the tetrahedral order parameter which approaches 1 for perfect tetrahedral coordination ( $109.47^\circ$  angles) and 0 for disordered arrangements.

For dynamical analysis, the **mean squared displacement** (MSD) is a critical quantity that tracks how far atoms move over time. It is given by

$$\text{MSD}(t) = \frac{1}{N} \sum_{i=1}^N \langle |\mathbf{r}_i(t) - \mathbf{r}_i(0)|^2 \rangle,$$

where  $\mathbf{r}_i(t)$  is the position of atom  $i$  at time  $t$ , and the average is taken over all atoms. The MSD provides insights into diffusive behavior in materials. `fastatomstruct` uses the very efficient `tidynamics` Python library (Buyl, 2018) to calculate the time-averaged MSD. The non-averaged MSD is implemented in `fastatomstruct` itself through direct calculation of displacement vectors for each atom at each time step, followed by squared magnitude computation and ensemble averaging.

The **non-Gaussian parameter** (NGP) measures deviations from Gaussian diffusion and is defined as

$$\alpha_2(t) = \frac{\frac{1}{N} \sum_{i=1}^N \langle |\mathbf{r}_i(t) - \mathbf{r}_i(0)|^4 \rangle}{\left( \frac{1}{N} \sum_{i=1}^N \langle |\mathbf{r}_i(t) - \mathbf{r}_i(0)|^2 \rangle \right)^2} - 1.$$

This parameter is particularly useful for identifying heterogeneities in atomic motion.

The (coherent) **intermediate scattering function** describes the decay of the density fluctuations in the system. It is given by the Fourier-transform of the autocorrelation function of the particle density,

$$F(\mathbf{q}, t) = \frac{1}{N} \sum_{i,j} \langle \exp [i\mathbf{q} \cdot (\mathbf{r}_i(t) - \mathbf{r}_j(0))] \rangle.$$

Note that  $S(\mathbf{q}) = F(\mathbf{q}, 0)$  for the static structure factor. The *incoherent* or *self*-part of the intermediate scattering function,

$$F_{\text{incoh}}(\mathbf{q}, t) = \frac{1}{N} \sum_i \langle \exp [i\mathbf{q} \cdot (\mathbf{r}_i(t) - \mathbf{r}_i(0))] \rangle,$$

captures only single-particle (diffusive) motion. The implementation computes the complex exponentials for displacement vectors at different time lags, performs the summation over particle pairs (coherent) or individual particles (incoherent), and averages over time origins.

The **overlap parameter** (Lačević et al., 2003)

$$Q(t) = \sum_{i,j=1}^N w(|\mathbf{r}_i(0) - \mathbf{r}_j(t)|)$$

is a simple but powerful tool to quantify the overlap of a configuration at time  $t$  with the reference configuration at  $t = 0$ . It gives the number of particles that either remained within their environment of size  $a$ , or were replaced by another particle. The extent of this region is introduced via the function  $w(x)$ , which is equal to one for  $x < a$ , and zero otherwise. The so-called self part is given by

$$Q_s(t) = \sum_{i=1}^N w(|\mathbf{r}_i(0) - \mathbf{r}_i(t)|).$$

The corresponding distinct part ( $i \neq j$ ) is usually small and only visible on very long timescales. The implementation uses spatial hashing to efficiently identify particle pairs within the overlap threshold distance, applies the step function criterion, and counts the overlapping particles for

both self and distinct contributions. We can now also define a **four-point susceptibility** that measures variability of  $Q$ ,

$$\chi_4(t) = \frac{\beta V}{N^2} \langle Q^2(t) \rangle - \langle Q(t) \rangle^2.$$

As explained by Lačević et al. (2003), this quantity can be related to the size of dynamically correlated regions. We can split it into three different contributions, the self part  $\chi_{ss}(t)$ , the distinct part  $\chi_{dd}(t)$ , and the cross part  $\chi_{sd}(t)$ , which are defined as

$$\begin{aligned}\chi_{ss}(t) &= \frac{\beta V}{N^2} \langle Q_s^2(t) \rangle - \langle Q_s(t) \rangle^2, \\ \chi_{dd}(t) &= \frac{\beta V}{N^2} \langle Q_d^2(t) \rangle - \langle Q_d(t) \rangle^2, \text{ and} \\ \chi_{sd}(t) &= \frac{\beta V}{N^2} \langle Q_s(t) Q_d(t) \rangle - \langle Q_s(t) \rangle \langle Q_d(t) \rangle.\end{aligned}$$

The distinct part and cross part almost completely cancel each other and thus only contribute minor corrections to the full four-point susceptibility.

The **velocity autocorrelation function** (VACF) describes how the velocity of an atom is correlated with itself over time and is given by

$$C_v(t) = \frac{1}{N} \sum_{i=1}^N \langle \mathbf{v}_i(0) \cdot \mathbf{v}_i(t) \rangle,$$

where  $\mathbf{v}_i(t)$  is the velocity of atom  $i$  at time  $t$ . VACFs provide information about vibrational modes. The implementation performs direct time-domain autocorrelation with optional mass weighting, computing the dot product of velocity vectors at different time lags and normalizing by the initial (zero-lag) value. The **vibrational density of states** (VDOS) can be derived either from a direct FFT of atomic velocities, or from the Fourier transform of the VACF. It gives the distribution of vibrational frequencies in a material. `fastatomstruct` closely follows the implementation of the `pwtools` Python library (Schmerler, 2025) to calculate the VDOS, but offers a direct interface with the Atomic Simulation Environment (ASE).

The **viscosity** can be calculated directly from the stress-stress autocorrelation function as (Cui et al., 1996)

$$\eta = \frac{V}{k_B T} \lim_{T \rightarrow \infty} \int_0^T \langle \sigma_{xy}(t') \sigma_{xy}(0) \rangle dt'.$$

`fastatomstruct` supports the calculation of this autocorrelation and viscosity from molecular dynamics simulations. The implementation follows the Green-Kubo relation by computing the stress tensor autocorrelation function and performing trapezoidal integration to obtain the running integral, which converges to the viscosity in the long-time limit.

Finally, we would like to note that parallelization is a core strength of the library. Thread-based parallelization using Rust's `rayon` library ensures efficient use of multicore processors, while image-based parallelization with MPI enables scalability to datasets with many different snapshots. Figure 3 shows the scaling behavior of different functions implemented in `fastatomstruct`. The library's compatibility with ASE and other Python-based tools further simplifies integration and usability for researchers. The Rust implementation has several advantages over more traditional approaches like combining Python with C or Fortran (Perkel, 2020). By design, Rust guarantees both memory and thread safety, which excludes entire classes of bugs that are common in other languages. In particular, Rust's ownership concept excludes race conditions, which makes it straightforward to write parallel code that is both fast and correct. The Rust compiler provides extensive static analysis, which can catch many bugs at compile time. As a result, `fastatomstruct` is a very robust and reliable library for structural and dynamical analysis of atomic systems. We hope that our approach using a



rather non-traditional language for scientific computing can inspire other works to adopt Rust for high-performance computing tasks. Besides the advantages over languages like C/C++ or Fortran mentioned above, Rust also offers modern tooling and easy integration with Python through the PyO3 crate, and it can be interfaced with existing C/C++ or Fortran code. Increasing usage of Rust should also improve the overall quality of scientific software by finding and eliminating common bugs very early in the development process.

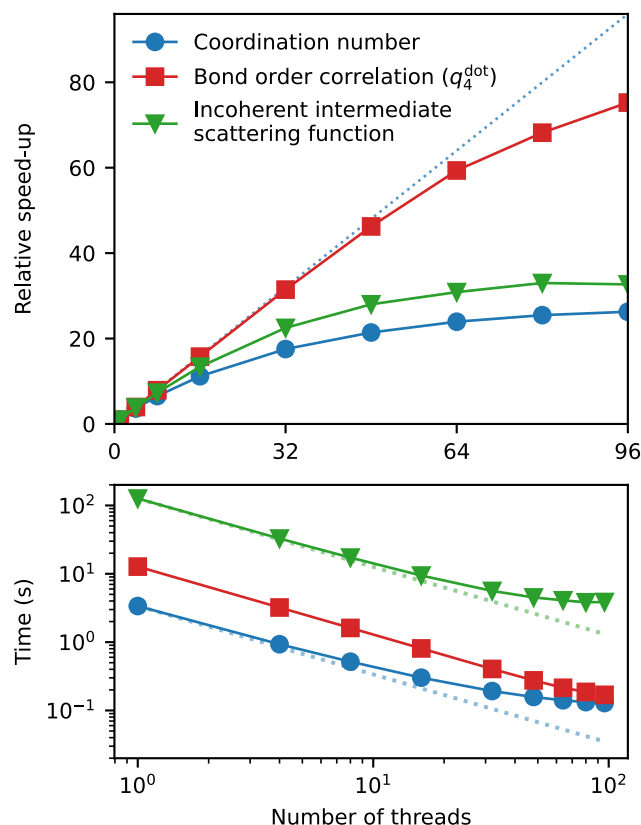


**Figure 3:** Scaling behavior of exemplary calculations with fastatomstruct. Relative speed-ups compared to a single thread (top) and total calculation times (bottom) are shown for calculations of coordination numbers, bond order correlation, and the incoherent intermediate scattering function. Tests have been performed on an AMD EPYC Genoa 9654 processor with 96 cores and threads. A system with 32,000 atoms was used for the calculation of the bond order correlation parameter  $q_4^{\text{dot}}$ . 256,000 atoms were used for coordination number calculations. The incoherent intermediate scattering function was calculated for 600 snapshots from a molecular dynamics simulation with 32,000 atoms. Scalability for large threads counts is limited because the calculations are memory bound, which holds for the intermediate scattering function calculations in particular. The repository contains an example (examples/perf\_intermediate\_scattering) to demonstrate this.



## Applications in Research

The `fastatomstruct` package enables the study of a wide range of structural and dynamical phenomena, while integrating well in many existing workflows based on the Atomic Simulation Environment (Hjorth Larsen et al., 2017). For instance, researchers can analyze phase transitions in amorphous materials by calculating bond-orientational parameters, which provide insights into changes in local atomic order. The library is particularly suited for studying the dynamics of supercooled liquids and glasses. This has been exploited in recent studies of liquid, supercooled-liquid and glassy antimony (Holle et al., 2025).

## Acknowledgments

We acknowledge support from the German Research Foundation (DFG) through the collaborative research centers Nanoswitches (SFB 917) and Intelligent Matter (SFB 1459) as well as the European Research Council (ERC-Grant No. 640003). RM acknowledges funding from the PRIN 2020 project “Neuromorphic devices based on chalcogenide heterostructures” funded by the Italian Ministry for University and Research (MUR). Calculations for this publication were performed on the HPC cluster PALMA II of the University of Münster, subsidized by the DFG (INST 211/667-1).

## References

- Bichara, C., Pellegatti, A., & Gaspard, J.-P. (1993). Properties of liquid group-V elements: A numerical tight-binding simulation. *Physical Review B*, 47(9), 5002–5007. <https://doi.org/10.1103/PhysRevB.47.5002>
- Buyl, P. de. (2018). Tidynamics: A tiny package to compute the dynamics of stochastic and molecular simulations. *Journal of Open Source Software*, 3(28), 877. <https://doi.org/10.21105/joss.00877>
- Cui, S. T., Cummings, P. T., & Cochran, H. D. (1996). The calculation of the viscosity from the autocorrelation function using molecular and atomic stress tensors. *Molecular Physics*, 88(6), 1657–1664. <https://doi.org/10.1080/00268979609484542>
- Duboué-Dijon, E., & Laage, D. (2015). Characterization of the Local Structure in Liquid Water by Various Order Parameters. *The Journal of Physical Chemistry B*, 119(26), 8406–8418. <https://doi.org/10.1021/acs.jpcb.5b02936>
- Friederich, P., Häse, F., Proppe, J., & Aspuru-Guzik, A. (2021). Machine-learned potentials for next-generation matter simulations. *Nature Materials*, 20(6), 750–761. <https://doi.org/10.1038/s41563-020-0777-6>
- Gowers, R. J., Linke, M., Barnoud, J., Reddy, T. J. E., Melo, M. N., Seyler, S. L., Domański, J., Dotson, D. L., Buchoux, S., Kenney, I. M., & Beckstein, O. (2016). MDAnalysis: A Python Package for the Rapid Analysis of Molecular Dynamics Simulations. *Scipy*. <https://doi.org/10.25080/Majora-629e541a-00e>
- Hjorth Larsen, A., Jørgen Mortensen, J., Blomqvist, J., Castelli, I. E., Christensen, R., Duřak, M., Friis, J., Groves, M. N., Hammer, B., Hargus, C., Hermes, E. D., Jennings, P. C., Bjerre Jensen, P., Kermode, J., Kitchin, J. R., Leonhard Kolsbjerg, E., Kubal, J., Kaasbjerg, K., Lysgaard, S., ... Jacobsen, K. W. (2017). The atomic simulation environment—a Python library for working with atoms. *Journal of Physics: Condensed Matter*, 29(27), 273002. <https://doi.org/10.1088/1361-648X/aa680e>
- Holle, N., Walfort, S., Ballmaier, J., Mazzarello, R., & Salinga, M. (2025). Importance of Density for Phase-Change Materials Demonstrated by Ab Initio Simulations of Amorphous

- Antimony. *Physical Review Letters*, 134(4), 046101. <https://doi.org/10.1103/PhysRevLett.134.046101>
- Lačević, N., Starr, F. W., Schröder, T. B., & Glotzer, S. C. (2003). Spatially heterogeneous dynamics investigated via a time-dependent four-point density correlation function. *The Journal of Chemical Physics*, 119(14), 7372–7387. <https://doi.org/10.1063/1.1605094>
- Lee, C., Vanderbilt, D., Laasonen, K., Car, R., & Parrinello, M. (1993). Ab initio studies on the structural and dynamical properties of ice. *Physical Review B*, 47(9), 4863–4872. <https://doi.org/10.1103/PhysRevB.47.4863>
- Michaud-Agrawal, N., Denning, E. J., Woolf, T. B., & Beckstein, O. (2011). MDAAnalysis: A toolkit for the analysis of molecular dynamics simulations. *Journal of Computational Chemistry*, 32(10), 2319–2327. <https://doi.org/10.1002/jcc.21787>
- Ong, S. P., Richards, W. D., Jain, A., Hautier, G., Kocher, M., Cholia, S., Gunter, D., Chevrier, V. L., Persson, K. A., & Ceder, G. (2013). Python Materials Genomics (pymatgen): A robust, open-source python library for materials analysis. *Computational Materials Science*, 68, 314–319. <https://doi.org/10.1016/j.commatsci.2012.10.028>
- Perkel, J. M. (2020). Why scientists are turning to Rust. *Nature*, 588(7836), 185–186. <https://doi.org/10.1038/d41586-020-03382-2>
- Ronneberger, I., Mazzarello, R., & Wuttig, M. (2016). *Computational Study of Crystallization Kinetics of Phase Change Materials* [PhD thesis, RWTH Aachen University]. <https://doi.org/10.18154/RWTH-2017-00376>
- Schmerler, S. (2025). *Elcorto/pwtools*. <https://doi.org/10.5281/zenodo.13128303>
- Steinhardt, P. J., Nelson, D. R., & Ronchetti, M. (1983). Bond-orientational order in liquids and glasses. *Physical Review B*, 28(2), 784–805. <https://doi.org/10.1103/PhysRevB.28.784>
- ten Wolde, P. R., Ruiz-Montero, M. J., & Frenkel, D. (1995). Numerical Evidence for bcc Ordering at the Surface of a Critical fcc Nucleus. *Physical Review Letters*, 75(14), 2714–2717. <https://doi.org/10.1103/PhysRevLett.75.2714>